WATER VAPOR PRESSURE DEPENDENCE OF CRYSTALLIZATION OF AMORPHOUS ENSTATITE.
K. Kobayashi[1], D. Yamamoto[1] and S. Tachibana[1], [1]Department of Natural History Sciences, Hokkaido University, Sapporo, Hokkaido 060-0810, Japan. (kodai@ep.sci.hokudai.ac.jp).

Introduction: Silicate dust is dominant among solid materials in astronomical environments. Infrared spectroscopic observations of astronomical environments and mineralogical studies show that both crystalline and amorphous silicate dust are present in protoplanetary disks [e.g., 1 and reference therein], while silicate dust in the interstellar medium is mostly amorphous (crystalline fraction: ~0.2 %) [2]. This indicates that amorphous silicates transform into crystalline silicates due to thermal annealing in protoplanetary disks.

In order to investigate the dust evolution and constrain the condition, where crystallization of amorphous silicates takes place in protoplanetary disks, crystallization of amorphous silicates has been investigated experimentally using astronomical dust analogs under various conditions [e.g., 3]. One of those experiments [4] showed that the presence of hydroxyl group in amorphous structure significantly lowers the activation energy for crystallization. Moreover, crystallization experiments of forsterite under various water vapor pressure conditions suggests that crystallization of amorphous forsterite is promoted in the presence of water vapor [5]. However, the effect of water vapor on crystallization kinetics and mechanism of amorphous enstatite, of which Mg/Si ratio is close to the solar ratio, has not yet been understood in detail. Here we conducted crystallization experiments of amorphous enstatite under various water vapor pressure conditions to investigate the effect of water vapor on crystallization of amorphous enstatite.

Experiments: Sub-μm-sized amorphous enstatite powder synthesized by an induced thermal plasma method [6] was used as a starting material. Heating experiments were carried out at 780−850°C in air (P_{H2O}~10^{-3} bar), in vacuum (P_{H2O}~10^{-10}−10^{-9} bar) and at P_{H2O} ~10^{-5} bar for 0.5−168 hours. Experiments in vacuum were carried out using a gold-image vacuum furnace (Thermo-Riko GFA430VN). The vacuum furnace was pumped down to ~10^{-10}−10^{-9} bar, and a dominant gas species during experiments was found to be water vapor using a quadrupole mass spectrometer (MKS e-Vision+). Experiments at P_{H2O} ~10^{-5} bar were conducted using the same vacuum furnace equipped with a gas flow system. The water vapor pressure in the chamber was adjusted by a balance between the H_2O gas flow and pumping rates. Heating experiments in air were conducted in a muffle furnace.

Run products were ground in an agate mortar for 15 minutes and analyzed with a Fourier transform infrared spectrometer (JASCO FT-IR 4200) using a KBr pellet method. The samples were also examined by powder X-ray diffraction (Rigaku SmartLab). A sample heated in vacuum at 800℃ for 12 hours was observed with a transmission electron microscope (TEM) with kind help of Yuki Kimura at Inst. Low Temperature Science, Hokkaido University.

Results and Discussion: Infrared absorption spectra of samples heated at three different water vapor pressure conditions change gradually with heating duration from broad features of amorphous enstatite at 10 and 18 μm to prominent features of crystalline enstatite at 9.3, 9.9, 10.6, 11.1, 11.6, 15.4 and 18.2, 19.5 μm (Fig. 1). Quantitative analysis of crystallization degree was made based on the infrared spectral fitting of the 10-μm absorption feature. We confirmed that infrared spectra of run products heated for the longest duration underwent no further change, and thus used them as a crystalline enstatite reference spectrum at each temperature and water vapor pressure. The time evolution of the fraction of crystalline enstatite was fitted with the Johnson-Mehl-Avrami (JMA) equation [7, 8], where the time constant for crystallization and the Avrami parameter of *n* were obtained. The Avrami parameter *n* in the JMA equation is related to the phase transformation mechanism involving nucleation and growth processes.

The *n* was found to be ~2.5 in air, suggesting the three-dimensional diffusion-controlled growth with homogeneous nucleation. This is consistent with previous crystallization experiments of amorphous enstatite, synthesized by a sol-gel method and an induced thermal plasma method, in air [6, 9].

The crystallization rate in vacuum was larger at temperatures above ~780°C than that in air, and the obtained *n* was ~1.5, which suggests that three-dimensional diffusion-controlled growth of crystalline enstatite after heterogeneous nucleation. This was supported by TEM observations, where crystalline enstatite was only identified at the surface of the grains in the sample heated at 800°C in vacuum for a short duration (12 hours) (Fig. 2) although electron diffraction showed that the grains were almost amorphous. Selective evaporation of Mg and O from the grain surface in vacuum [10] might promote to form SiO_4 chain structures of SiO_4 tetrahedra at the surface, leading to heterogeneous nucleation of crystalline enstatite at the grain surface.

Crystallization of amorphous enstatite at P_{H2O} ~10^{-5} bar occured more rapidly than that in vacuum (Fig. 3),

indicating that water molecules diffusing into the amorphous structure cut atomic bonds and promotes the crystallization as in [5].

The activation energies of the reciprocal time constants obtained in air and in vacuum are ~589 kJ mol^{-1} and ~991 kJ mol^{-1}, respectively (Fig. 3), implying that the effective structural modification of amorphous network occurs with a less kinetic barrier due to water molecules diffusing into amorphous from air.

References: [1] Henning, Th. (2010) *Annu. Rev. of A&A,* 48, 21−46. [2] Kemper, F. et al. (2004) *ApJ,* 609, 826. [3] Hallenbeck, S. L. et al. (1989) *Icarus,* 131, 198-209. [4] Jäger, C. et al. (2003) *A&A,* 408, 193−204. [5] Yamamoto, D. (2016) *Master thesis*. [6] Imai, Y. (2012) *Ph.D. thesis*. [7] Avrami, M. (1939) *J. Chem. Phys.,* 7, 1103−1112. [8] Johnson, W. A. & Mehl, R. F. (1939) *Trans. Am. Inst. Min. Engin.*, 135, 416. [9] Murata, K. et al. (2009) *ApJ,* 697, 836-837. [10] Rietmeijer, F. J. M. et al. (1986) *Icarus,* 66, 211−222.

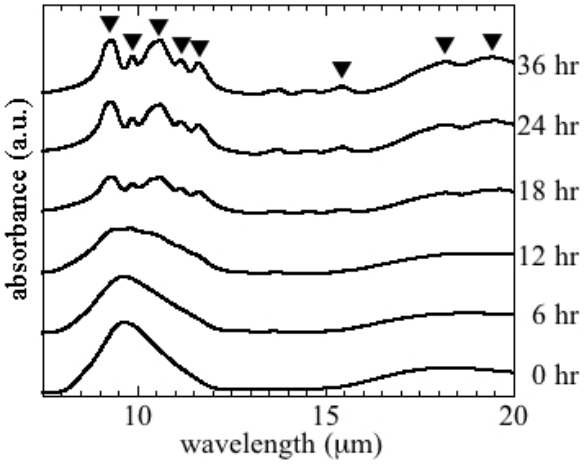

Fig. 1. Infrared absorption spectra of run products heated at 800°C in vacuum. Arrows represent prominent infrared absorption features of crystalline enstatite.

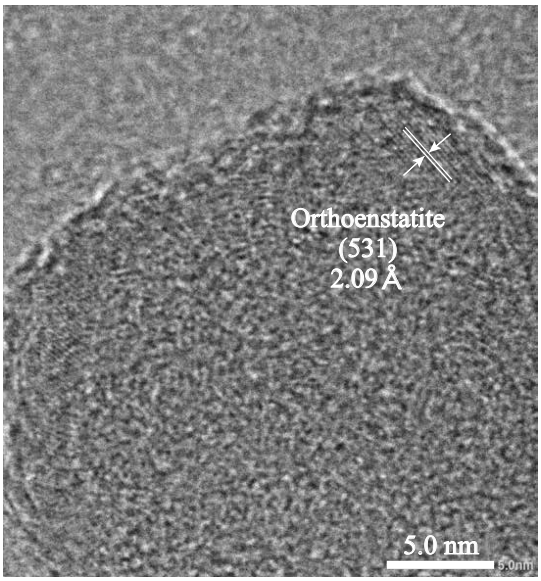

Fig. 2. A TEM image of the run product heated at 800°C in vacuum for 12 hours.

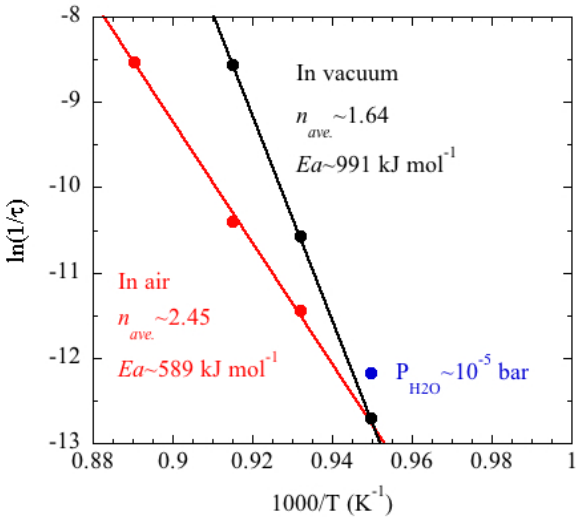

Fig. 3. Arrhenius plots of reciprocal time constants for crystallization of amorphous enstatite in air, in vacuum and at P_{H2O}~10^{-5} bar. Here *n* is the Avrami parameter and *Ea* is the activation energy.